RESTORING FORCE CHARACTERISTICS OF STEEL DIAGONAL BRACINGS

by Sadayoshi Igarashi(I), Kazuo Inoue(II),
Mitsugu Asano(III) and Koji Ogawa(III)

1. SYNOPSIS

In this paper, load-deformation relations and dynamic response characteristics of the steel X-bracing for the structural resistant component against earthquake are studied. First, nonlinear axial load-deformation relations of a bracing member subjected to cyclic axial force are defined under any given history of tension and/or compression. These axial load-deformation relations are employed to calculate load-deformation curves and dynamic response of X-braced structures, corresponding to various slenderness ratios of bracing members, and a comparison with Slip-Model(1) which is used as load-deformation relation of X-bracing is discussed.

2. NOTATIONS

A: Cross sectional area;
I: Sectional moment of inertia;
E: Young's Modulus;
L: Member length;
Λ: Slenderness ratio;
P: Axial force, positive in compression;
u: Axial deformation
M: Bending moment or mass of the system;
σy: Yield stress;
γ: Inclination of bracing;
x,y: Member coordinate axis;
Q: Restoring force;
X: Relative displacement of the mass;
To: Natural period of the system $(2\pi/\omega o)$;
Ar: Acceleration ratio; and
α: Maximum amplitude of ground acceleration.

3. INTRODUCTION

When a braced structure is subjected to an earthquake, a bracing member is likewise subjected to tension and/or compression alternatively. Under compressive force, an axial load carrying capacities and rigidities of such members are much decreased due to instability effects. Therefore, so called Slip-Model, neglecting the compressive strength of the member, has been used as the dynamic model of the braced frames.(2)-(4)

However, some recent theoretical and experimental studies(5)-(10) concerning a bracing member indicate that the effect of the compressive strength and rigidity upon the hysteretic behavior of an elasto-plastic bracing member under cyclic axial loading cannot be negligible in the smaller range of the slenderness ratio.

In this paper, we extended the concept of plastic hinge to include plastic deformation, both rotation and contraction, under combination of bending moment and axial force, following the plastic flow law, and derived the axial stiffness coefficients which define the relations between the incremental axial deformation and the incremental axial force in the elastic plastic range. The hysteretic characteristics of bracing members and X-braced structures presented. And these stiffness coefficients are

(I) Professor, (II) Assistant and (III) Graduate Student of Department of Architectural Engineering, Osaka University, Japan

employed to calculate dynamic response of one degree-of-freedom system of X-braced structure, subjected to earthquake motions corresponding to sinusoidal excitation and El-Centro 1940, N-S Component. The structural parameters considered in this study are the slenderness ratios of a bracing member and the natural periods of the system. The influences of the slenderness ratio on the response of X-braced structures are investigated, and a comparison with Slip-Model is also discussed to show the limitation that permits the application of Slip-Model.

4. ANALYTICAL METHOD OF A BRACING MEMBER

4.1 ASSUMPTIONS

The assumptions used for the analysis of a bracing member are as follows:

1° The member is taken as a one-dimensional continuum with both ends simply supported, and strains are distributed linearly through the depth of a section.

2° The stress-strain relation is perfectly elasto-plastic.

3° The compressive strength (Pcr) is defined as follows:

$$Pcr = \text{Min.}(Pe, Py)$$

in which Pe is Eulers load. The compressive strength remains untill the yield condition is satisfied.

4° The member is straight at first loading and after tensile yielding. The lateral deflection takes place when the compressive axial force reaches Pcr, and no local instability takes place.

5° The yield condition is considered under combined action of an axial force (P) and a bending mement (M). But shear effects are negligible. That is

$$\left|\frac{M}{Mp}\right| + \left(\frac{P}{Py}\right)^2 = 1$$

in which Mp is the plastic moment in pure bending and Py the yield load in pure tention.

6° The rotation and the elongation or the contraction at the plastic hinge are rigid-plastic.

7° An axial deformation consists of three components.

$$u = ue + ub + up$$

in which ue is due to elastic axial deformation, ub to bowing and up to plastic axial deformation at yield hinge.

4.2 AXIAL LOAD-DEFORMATION RELATIONS OF A BRACING MEMBER

According to above assumptions, an axial load-deformation relation of a bracing member shown in Fig.1 subjected to cyclic axial force is analyzed. Herein, an axial load-deformation relation is devided into following seven states as shown in Fig.2, namely

STATE-I : A member is straight and behaves elastically;
STATE-II : Elastic deformed state of the post-buckling;
STATE-III : Compressive mechanism line, that is, the plastic hinge has been formed at the center of a member;
STATE-IV : Compressive elastic range during unloading;
STATE-V : Tensile elastic range during unloading;
STATE-VI : Tensile mechanism lines and

STATE-VII : Tensile yield state.

The relations between the incremental axial force and the incremental axial deformation on each state are derived. In the derivation of these relations, the introduction of the following nondimensional quantities are considered.

$$p = \frac{P}{Py}\ ,\quad pe = \frac{Pe}{Py}\ ,\quad m = \frac{M}{Mp}\ ,\quad \delta = \frac{u}{L}\cdot\frac{EA}{Py}\ ,\quad \xi = \frac{2x}{L}\ ,$$
$$\eta = \frac{Py}{Mp}\cdot y\ ,\quad a = \frac{A}{I}\left(\frac{Mp}{Py}\right)^2\ ,\quad \nu = \frac{\pi}{2}\sqrt{\frac{|p|}{pe}}\ ,\quad \lambda = \frac{\Lambda}{\pi}\sqrt{\frac{\sigma y}{E}}\ . \tag{1}$$

in which, the parameter a is a number depending only on the shape of the cross-section. For a rectangular cross-section, $a = 0.75$. And λ is slenderness ratio nondimensionalized by the critical slenderness ratio, which implies that Λ is about 93 times as many as λ when σy is equal to $2.4 t/cm^2$ and E to $2100 t/cm^2$.

Now, the equilibrium differential equation of a bracing member of Fig.1 is given as follows using the relations shown in Eqs.(1).

$$\eta'' + \nu^2\eta = 0 \tag{2}$$

in which, prime denote the differentiation with respect to ξ. Using the boundary conditions, $\eta|_{\xi=0}=\eta m$ and $\eta|_{\xi=1}=0$, Eq.(2) is solved as follows:

$$\eta = \eta m[\cos(\nu\xi) - \cot\nu\cdot\sin(\nu\xi)] \tag{3}$$

The flexural shortening due to bowing (δb) is given by the following relation using Eq.(3).

$$\delta b = \frac{2a}{\pi^2\lambda^2}\int_0^1(\eta')^2 d\xi = \frac{a\eta_m^2\nu^2}{\pi^2\lambda^2}\left(\frac{1}{\sin^2\nu} + \frac{\cot\nu}{\nu}\right) \tag{4}$$

When the axial force is tensile, p is negative, and the trigonometric functions in Eqs.(3) and (4) have to be replaced by the corresponding hyperbolic functions.

The yield condition indicated in assumption 5° is nondimensionalized using Eqs.(1), namely

$$\phi = |m| + p^2 - 1 = |\eta m\cdot p| + p^2 - 1 = 0 \tag{5}$$

In conforming with assumption 7°, axial stiffness is given by the relation

$$k = \frac{dp}{d\delta} = 1\Big/\left(\frac{d\delta e}{dp} + \frac{d\delta b}{dp} + \frac{d\delta p}{dp}\right) \tag{6}$$

in which, $d\delta e/dp$ is equal to unity, and δp is nondimensional expression of up.

Using the above equations, axial stiffness is obtained as follows:

(1) STATE-I

$\delta b = \delta p = 0$

hence $k = 1 \qquad (-1 \leqq p \leqq \text{Min.}(pe,1))$ (7)

(2) STATE-II

$p = pcr = \text{const.}$

hence $k = 0$ (8)

(3) STATE-III

In this state, the yield condition is satisfied, therefore, the following relation is obtained using Eqs.(4) and (5).

$$\frac{d\delta b}{dp} = \frac{\partial \delta b}{\partial \eta m}\cdot\frac{d\eta m}{dp} + \frac{\partial \delta b}{\partial \nu}\cdot\frac{d\nu}{dp}$$

$$= \frac{a\eta m\nu^2}{\pi^2\lambda^2}\left\{2\left(\frac{1}{\sin^2\nu} + \frac{\cot\nu}{\nu}\right)\frac{d\eta m}{dp} + \eta m\left(\frac{\cot\nu}{\nu^2} + \frac{1}{\nu\sin^2\nu} - \frac{2\cos\nu}{\sin^3\nu}\right)\frac{d\nu}{dp}\right\} \qquad (9)$$

in which, from Eqs.(1) and (5)

$$\frac{d\nu}{dp} = \frac{\nu}{2p}, \qquad \frac{d\eta m}{dp} = -\frac{1}{|p|}\left(p + \frac{1}{p}\right) \qquad (10)$$

Next, according to the plastic flow law, plastic deformation components ($d\delta p$, $d\theta p$) are defined as follows:

$$d\delta p = \mu\frac{\partial \phi}{\partial p}, \qquad d\theta p = \mu\frac{\partial \phi}{\partial m} \qquad (11)$$

in which, μ is an arbitrary positive scalar. And plastic hinge rotation θp is given as

$$\theta p = 2\eta'\big|_{\xi=0} = 2\eta m\nu\cot\nu \qquad (12)$$

Eliminating μ from Eqs.(11) and using Eq.(12), the following relation is obtained.

$$\frac{d\delta p}{dp} = \left(\frac{\partial \phi}{\partial p}\Big/\frac{\partial \phi}{\partial m}\right)\cdot\frac{d\theta p}{dp} = \left(\frac{\partial \phi}{\partial p}\Big/\frac{\partial \phi}{\partial m}\right)\cdot\left(\frac{\partial \theta p}{\partial \eta m}\cdot\frac{d\eta m}{dp} + \frac{\partial \theta p}{\partial \nu}\cdot\frac{d\nu}{dp}\right)$$

$$= \frac{8ap}{\pi^2\lambda}\left\{\nu\cot\nu\cdot\frac{d\eta m}{dp} + \eta m\left(\cot\nu - \frac{\nu}{\sin^2\nu}\right)\frac{d\nu}{dp}\right\} \qquad (13)$$

Stiffness k is obtained by substituting Eqs.(9), (10) and (13) into Eq.(6).

(4) STATE-IV

In this state, the plastic hinge rotation θp at unloading is retained. Therefore, using Eqs.(4) and (12), the following relation is obtained.

$$\frac{d\delta b}{dp} = \frac{a\theta p^2}{4\pi^2\lambda^2}\left(\frac{2\sin\nu}{\cos^3\nu} - \frac{\tan\nu}{\nu^2} + \frac{1}{\nu\cos^2\nu}\right)\frac{d\nu}{dp}, \qquad \frac{d\delta p}{dp} = 0 \qquad (14)$$

Stiffness k is obtained by substituting Eqs.(14) into Eq.(6).

(5) STATE-V

Since axial force only change its sign, a similar manipulation in STATE-IV gives following relations.

$$\frac{d\delta b}{dp} = \frac{a\theta p^2}{4\pi^2\lambda^2}\left(-\frac{2\sinh\nu}{\cosh^3\nu} - \frac{\tanh\nu}{\nu^2} + \frac{1}{\nu\cosh^2\nu}\right)\frac{d\nu}{dp}, \qquad \frac{d\delta p}{dp} = 0 \qquad (15)$$

(6) STATE-VI

A similar manipulation in STATE-III gives following relations.

$$\frac{d\delta b}{dp} = \frac{a\eta m\nu^2}{\pi^2\lambda^2}\left\{2\left(\frac{1}{\sinh^2\nu} + \frac{\coth\nu}{\nu}\right)\frac{d\eta m}{dp} + \eta m\left(\frac{\coth\nu}{\nu^2} + \frac{1}{\nu\sinh^2\nu} - \frac{2\cosh\nu}{\sinh^3\nu}\right)\frac{d\nu}{dp}\right\} \qquad (16)$$

$$\frac{d\delta p}{dp} = -\frac{8ap}{\pi^2\lambda^2}\left\{\nu\coth\nu\cdot\frac{d\eta m}{dp} + \eta m\left(\coth\nu - \frac{\nu}{\sinh^3\nu}\right)\frac{d\nu}{dp}\right\} \tag{17}$$

And the plastic hinge rotation θp is given by the relation

$$\theta p = 2\eta m\nu\coth\nu \tag{18}$$

(7) STATE-VII

$$p = 1 = \text{const.}$$

hence $$\dot{k} = 0 \tag{19}$$

5. RESPONSE CALCULATIONS

The analysis is made, first, to illustrate the behavior of X-braced structure, shown in Fig.3, under cyclic horizontal loading on the column top. Second, dynamic response analysis is done by means of hereunder stated procedures.

The nondimensional undamped equation of motion of one degree-of-freedom system can be written in the form;

$$x'' + q = -Ar\cdot Xg'' \tag{20}$$

where

$$x = \frac{X}{Xy}\ ,\quad q = \frac{Q}{Qy}\ ,\quad K = \frac{Qy}{Xy}\ ,\quad \omega_0^2 = \frac{K}{M}\ ,\quad \tau = \omega_0 t$$

$$Ar = \frac{M\alpha}{Qy}\ ,\quad \ddot{X}g = \alpha\ddot{X}g \quad (|\ddot{X}g| \leq 1) \tag{21}$$

in which dots denote differentiation with respect to t, and prime to τ.

In Eqs.(21), adapting the horizontal component of Uy and Py of a bracing member to Xy and Qy, respectively, and rewriting,

$$x = \frac{X}{Xy} = \frac{2u/\cos\gamma}{2uy/\cos\gamma} = \frac{u}{uy} = \delta$$

$$q = \frac{Q}{Qy} = \frac{-Pt\cdot\cos\gamma + Pc\cdot\cos\gamma}{Py\cdot\cos\gamma} = -pt + pc \tag{22}$$

Therefore, by adapting Eqs.(22) to Eq.(20), the response analysis of X-braced structure is done regardless of γ.

Input energy (Ie), kinetic energy (Ke) and dissipated energy in plastic deformation and strain energy (De) nondimensionalized by elastic energy capacity of the structure (1/2·XyQy) are as follows:

$$Ie = -2Ar\int qXg'd\tau$$

$$Ke = (x' + ArXg')^2 \tag{23}$$

$$De = 2\int qdx$$

The equation of motion is solved by means of the mid-acceleration method, and the stiffness of a bracing member is assumed to respond linearly within each time interval.

6. PARAMETERS

The structural parameters considered in this analysis are the non-

dimensional slenderness ratio (λ) of a bracing member and the natural period of the system (To). The complete range of these parameters are as follows:

λ = 0.5, 1.0, 1.5, 2.0, 2.5 and 3.0, To = 0.5, 1.0, 1.5 and 2.0 (Sec.)

Two types of acceleration wave forms are adapted as typical excitation pattern to the structure; one type is 2 cosine waves coincident with the natural frequency of the structure, the other is the first 15 seconds acceleration of El-Centro earthquake, May 18, 1940, N-S component. And the value of Ar is equel to 2.0.

7. ANALYTICAL RESULTS

7.1 LOAD DEFORMATION RELATION UNDER CYCLIC HORIZONTAL LOADING

Figs.4(a),(b) and (c) show the p-δ, p-ηm and p-m relations of a bracing member in the case of λ = 1.5, respectively, in which the same number enclosed with circle indicates the corresponding history for δ, ηm and m, against the same axial force (p). It is instructive to illustrate the present method.

Fig.5 indicate q-x relations of X-braced structure when the displacement amplitude increases gradually under horizontal loading, correspondingly λ = 0.5, 1.5 and 2.5. Reffering to Figs.5, as λ becomes great, the hysteretic characteristics resembles Slip-Model, in shape.

7.2 DYNAMIC RESPONSE AGAINST COSINE WAVE

Table-1 indicates the maximum displacement for the case inputted the sinusoidal excitation and Fig.6 indicate the maximum displacement amplitude normalized by the maximum displacement amplitude of Slip-Model. Reffering to Fig.6, as λ becomes great, the maximum displacement increases also, and in the range of $\lambda \geq 2.0$, the response becomes constant, that is, approaches the response of Slip-Model.

Fig.7 indicates De normalized by De of Slip-Model, correspondingly to different λ. It shows that as λ becomes great, De tends to unity decreasingly, that is, the loop area of the hysteretic response curve becomes small according to resemblance Slip-Model.

7.3 DYNAMIC RESPONSE AGAINST EARTHQUAKE

Table-2 indicates the maximum displacement for different λ and To against El-Centro earthquake input. Reffering to this, except for the case of To = 1.5, as To becomes small or λ becomes great, the responses increase. For example, Figs.8(a)-(f) show the hysteretic response curves in the case of To = 1.0, correspondingly different λ, in which the numerals indicate the time (sec.). They well document the transition to Slip-Model. Moreover, due to decreasing compressive strength of a bracing member, the maximum strength of the structure decreases gradually also, but the maximum displacement becomes great conversely.

Fig.9 indicates displacement response curves for different λ, in the case of To = 1.0. As λ becomes great, its shape tends to resemble the response curve of Slip-Model.

Figs.10 and 11 indicate the maximum displacement normalized by the maximum displacement of Slip-Model. Reffering to these, as λ becomes great, the responses tend to unity, particularly $\lambda \geq 2.0$, except for To = 1.5, near-

ly equel to unity. In the small range of λ, as To becomes small, the difference to Slip-Model is remarkable. That is, the maximum displacement response is much influenced by λ, in the small range of To.

8. CONCLUSION REMARKS

In this study, the effect of the slenderness ratio of a bracing member upon the restoring force characteristics and the inelastic response of steel X-braced structures were investigated. And the following results appeared significantly;

1. Inelastic behavior of X-braced structure was much influenced by the slenderness ratio of a bracing member, that is, it is inadequate to neglect the compressive strength and rigidity in smaller range of λ.
2. It is considered that the Slip-Model is applicable to X-braced structures in the range the nondimensional slenderness ratio is greater than 2.0.

BIBLIOGRAPHY

(1) R. Tanabashi and K. Kaneta, On the relation between the restoring force characteristics of structures and the pattern of earthquake ground motions, Proceedings of Japan National Symposium on Earthquake Engineering, 1962
(2) A.S. Veletsos, Maximum deformations of certain nonlinear systems, 4WCEE, 1969
(3) R.D. Hanson and W.R.S. Fan, The effect of minimum cross bracing on inelastic response of multi-story building, 4WCEE, 1969
(4) G.H. Workman, The inelastic behabior of multistory braced frame structures subjected to earthquake excitation, Thesis of the University of Michigan Department of Civil Engineering, 1969
(5) M. Wakabayashi and B. Tsuji, Experimental investigation on the behavior of frames with and without bracing under horizontal loading, Bulletin, Disaster Prevention Research Institute, Kyoto University, Vol.16, Part 2, No.112, Japan, 1967
(6) T. Nonaka, An elasto-plastic analysis of a bar under repeated axial loading, Submitted to Int. Journal of Solids and Structures.
(7) M. Yamada and B. Tsuji, A study on elasto-plastic deformation characteristics of brace under cyclic axial loading (II , A comparison analytical results with experimental results), Abstracts, Annual Meeting of Architectural Institute of Japan, 1972 (in Japanese)
(8) J. Sakamoto and Y. Obama, An analytical consideration for elasto-plastic hysteretic characteristics of steel brace element, Abstracts, Annual Meeting of Architectural Institute of Japan, 1972 (in Japanese)
(9) N. Fujimoto, A. Wada, K. Shirakata and R. Kosugi, A study on elasto-plastic characteristics of steel braced frame under cyclic horizontal loading, (Part VI. Theoretical analysis using the strain hardening model-II), Abstracts, Annual Meeting of Architectural Institute of Japan, 1972 (in Japanese)
(10) S. Igarashi, K. Inoue, M. Kibayashi and M. Asano, Restoring force characteristics of steel braced frames (Part I. The behavior of a bracing member under cyclic axial loading), Transactions of the Architectural Institute of Japan, No.196, Jun., 1972 (in Japanese)

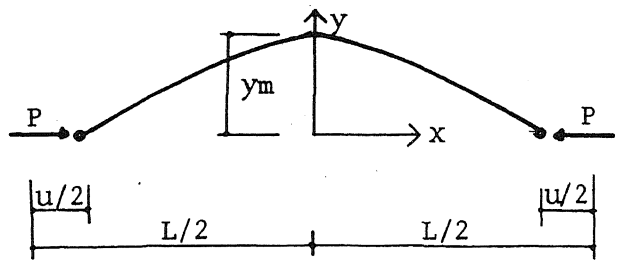

Fig.1 Deflected bracing member

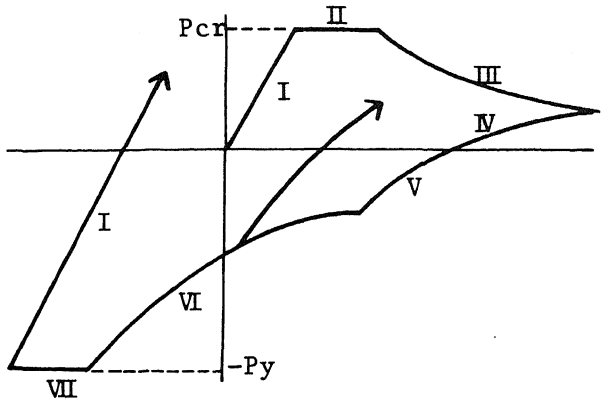

Fig.2 State No. of hysteresis curve of a bracing member

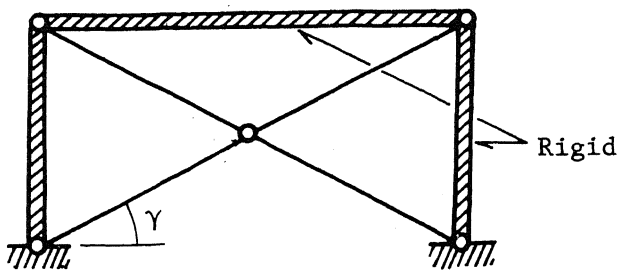

Fig.3 Idealized model of X-braced structure

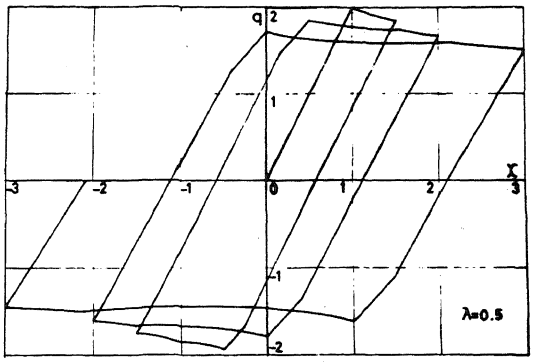

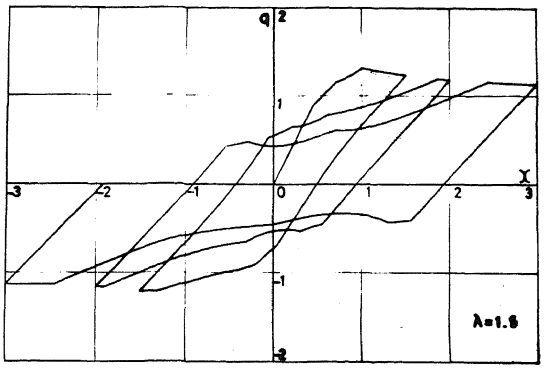

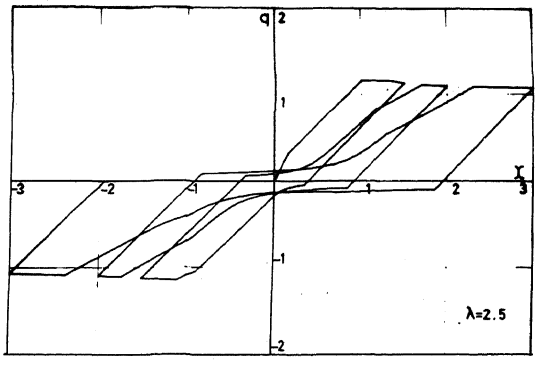

Fig.5 q-X relations of X-braced structure

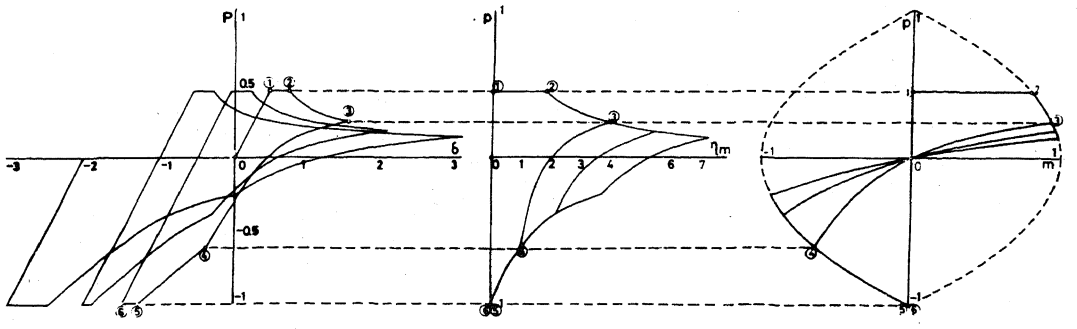

(a) p-δ relation (b) p-ηm relation (c) p-m relation

Fig.4 Behavior of a bracing member under cyclic axial force (λ=1.5)

λ	0.5	1.0	1.5	2.0	2.5	3.0	Slip
Xmax	7.01	7.58	8.26	8.44	8.52	8.58	8.32

Table-1 Maximum displacement amplitude (cosine input)

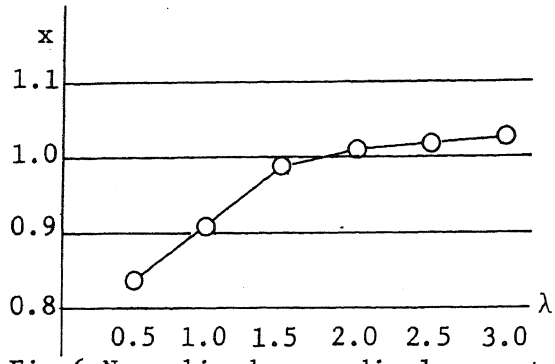

Fig.6 Normalized max. displacement amplitude (cosine input)

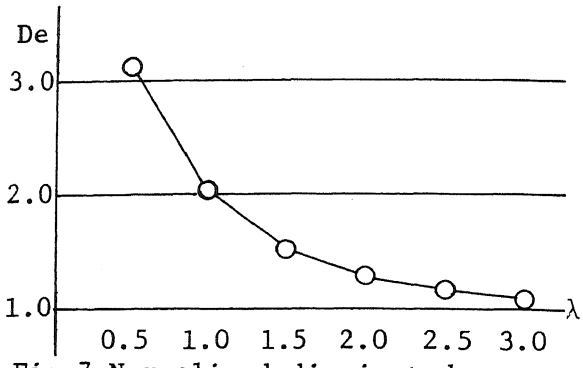

Fig.7 Normalized dissipated energy (cosine input)

To \ λ	0.5	1.0	1.5	2.0	2.5	3.0	Slip
0.5	4.00	6.16	-10.83	-19.18	-19.65	-19.82	-18.25
1.0	-2.63	-2.45	-3.15	-4.16	-4.75	-5.28	-5.09
1.5	1.56	-1.42	-1.45	-1.34	-1.29	1.11	1.89
2.0	1.00	1.00	-0.78	-1.16	-1.28	1.20	1.26

Table-2 Maximum displacement (El-Centro input)

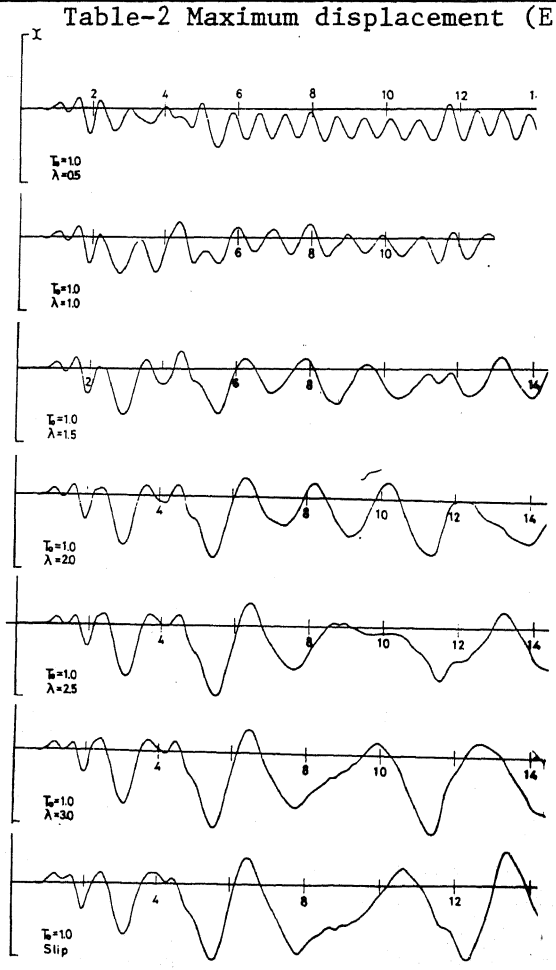

Fig.9 Displacement response (El-Centro input)

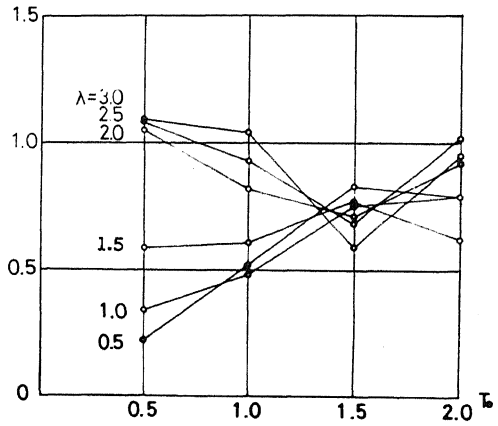

Fig.10 Normalized max. displacement (El-Centro input)

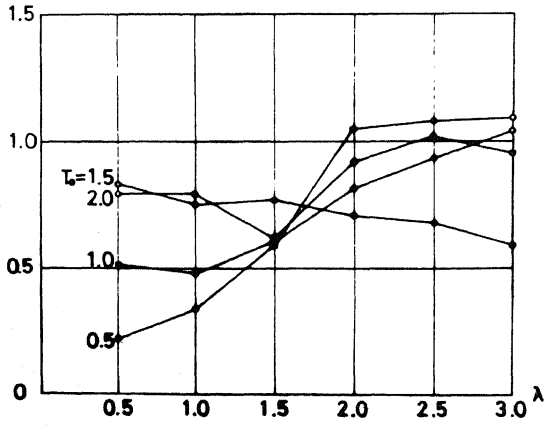

Fig.11 Normalized max. displacement (El-Centro input)

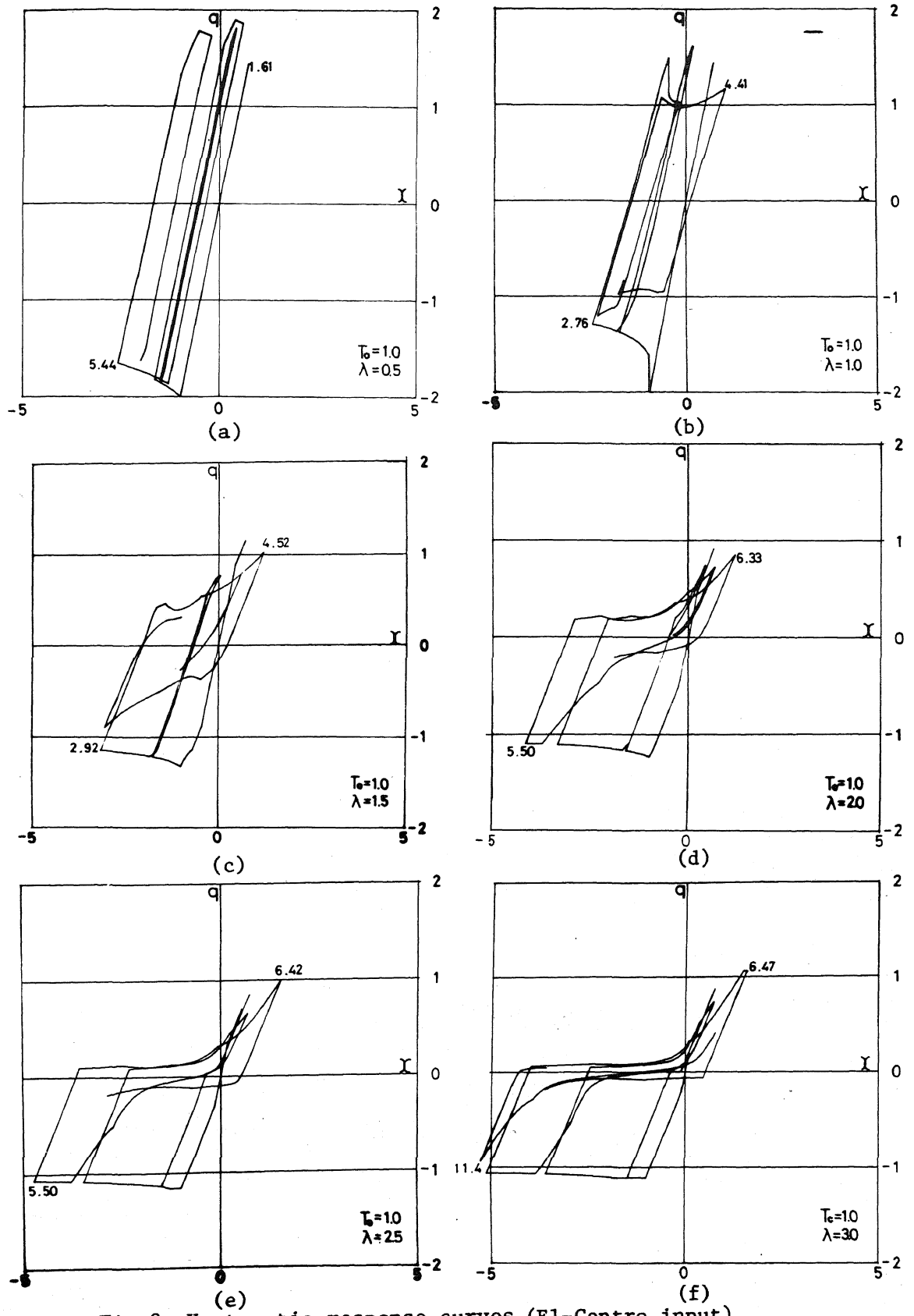

Fig.8 Hysteretic response curves (El-Centro input)